Heating Power Ratio Calculation to Design Test Section Including Non-Heated Side Wall

Kiwon Song[a*], Hyung Min Son[a], Jongharк Park[a]
[a]Korea Atomic Energy Research Institute, 989-111 Daedeok Daero, Yuseong Gu, Daejeon, 305-353, Korea
[*]Corresponding author: k1song@kaeri.re.kr

1. Introduction

Plate-type fuel assembly is composed of several thin-gap channels partitioned by plate-type fuels. Plate-type fuel is generally inserted in a frame which doesn't generate heat. Various CHF experiments in a narrow rectangular channel have been carried out [1, 2, 3]. KAERI has designed channel for plate-type fuel which includes heated wall and non-heated side wall simulating a frame [4]. Since direct heating is applied to the entire channel, non-heated side wall is made of the material with relatively high electrical resistance to reduce heat generation. This paper estimates the amount of heat generation at non-heated wall by using CFX code. This study is helpful to design test section including non-heated side wall using direct heating method.

2. Heating Power Calculation Method

The cross section of the test channel is depicted in Fig. 1. Non-heated side wall made of SUS304 is welded onto S45C heated plate. The channel length is 600 mm with 2.35 mm gap.

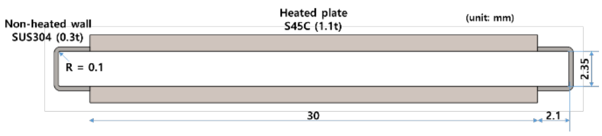

Fig. 1. Cross section of the test channel

Table I shows the material properties of the non-heated wall and heater plate. Since heated plate and non-heated wall has parallel connection to voltage direction, higher resistance yields lower power based on the equation (1).

$$P = \frac{V^2}{R} \quad (1)$$

Where, P is power(W), V is voltage(V) and R is resistance(Ω).

Material thickness of non-heated wall is designed thinner than heated plate to generate power as low as possible.

Table I: Material properties [5]

Material	Thermal Conductivity	Electrical Resistance	Specific Heat Capacity	Density
	W/(m·K)	μΩ·m	J/(kg·K)	kg/m³
SUS304	16.8	0.72	490	8,000
S45C	49.8	0.41	486	7,850

Generated power ratio is calculated in table II. Since the value of the heat flux does not affect its distribution, target heat flux is assumed 3,950 kW/m². Required electrical potential was estimated 23 V to generate target heat flux. This calculation doesn't consider heat conduction between two materials assuming that thermal contact resistance is very high. As a result, 3.49 % of total power is generated at non-heated wall.

Table II: Power ratio calculation

Heater Plate (S45C)					Non-heated (SUS304)						Entire Channel	Non-heated	-		
Length	Thick -ness	Width	Specific Resist -ance	Resist -ance	Length	Thick -ness	Gap Thick -ness	Width	Specific Resist -ance	Resist -ance	Resist -ance	power ratio	Target Heat Flux	Vol-tage	Current
(mm)	(mm)	(mm)	(μΩ·m)	(Ω)	(mm)	(mm)	(mm)	(mm)	(μΩ·m)	(Ω)	(Ω)	-	(kW/m²)	(V)	(A)
600	1.1	30	0.41	0.0075	600	0.3	2.35	4.2	0.72	0.22	0.0036	3.49%	3,950	23.0	6,386

3. CFX Calculation for Heating Power Ratio for Test Channel

Fig. 2 shows the boundary condition for CFX calculation. 23 V voltage is given to both end of the 600 mm channel to generate thermal power. Inside of the channel is cooled with 50,000 W/(m²·K), while outside of the channel is adiabatic. Since the value of heat transfer coefficient has effect on the absolute value of the wall temperature, but has no effect on temperature distribution, heat transfer coefficient was arbitrarily decided. For a similar reason, 80 ℃ ambient temperature was chosen.

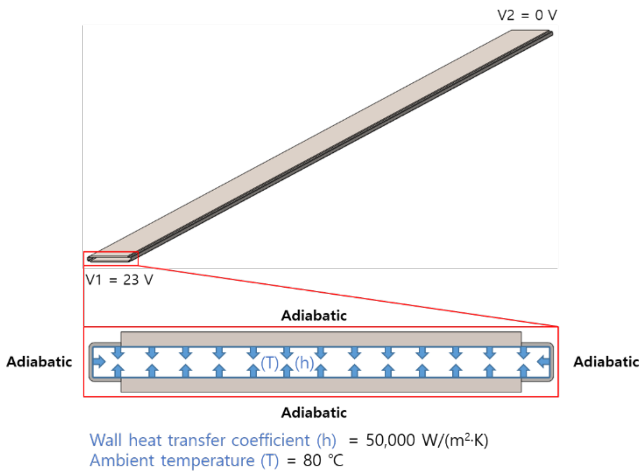

Fig. 2. Boundary condition for CFX calculation

There are conduction heat transfer through contact surfaces between heated plate and non-heated wall. In this study, two cases of calculation was carried out: maximum thermal contact resistance, and zero thermal contact resistance.

The heat flux distribution along the channel width direction is described in Fig. 3. High and uniform heat flux is applied from the center of the heater plate to near non-heated wall. In maximum thermal contact resistance case, heat flux falls steeply at contact surface, while heat flux falls slowly in zero thermal contact resistance case.

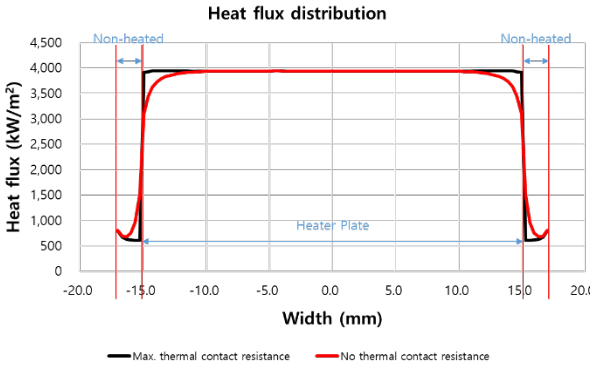

Fig. 3. Surface heat flux distribution along the channel width

Since heater plate material S45C has the higher thermal conductivity, heat flux at heater plate can easily be uniform distribution. On the other hand, less heat is transferred to non-heated wall due to the low thermal conductivity of SUS304, which is fit for purpose of the test section design. Slightly higher heat flux is observed at the end of the non-heated wall, because higher current density is found at the curved side wall.

Table III: Calculation results

	Total power (kW)	Heat generation at heater plate (kW)	Heat generation at non-heated wall (kW)	Heat generation ratio at non-heated wall
Hand Calculation	142.2	137.2	5.0	3.49 %
CFX–No thermal contact resistance	146.1	139.4	6.8	4.63 %
CFX–Max. thermal contact resistance	146.1	141.1	5.1	3.46 %

Calculation results are compared to each other in table III. Without considering of conduction heat transfer at contact surface, heat generation (power) ratio at non-heated wall to total is estimated 3.49 % and 3.46 % at hand calculation and CFX calculation respectively. Based on this result, hand calculation can be regarded as reliable. In no thermal contact resistance case, 4.63 % of the total heat is generated at non-heated wall, which is 1.17% higher than maximum thermal contact resistance case. This 1.17% heat can be considered as the amount of conduction heat transfer through contact surface. Therefore, this study can conclude that minimum 3.46 % to maximum 4.63 % of heat can be generated at non-heated side wall in direct heating experiment.

4. Summary

This paper presents the calculation results of the heat power ratio at test section including non-heated side wall. Regardless of conduction heat transfer at contact surface, hand calculation has very similar result with CFX code calculation. Considering of conduction heat transfer at contact surface, 1.17 % higher heat is generated.

This study shows that 3.46 % to 4.63 % of the heat is generated at non-heated side wall in 30 mm heater plate test section.

ACKNOWLEDGEMENT

This work was supported as a part of the Technology Development and Enhancement for Supporting the Export of Research Reactor Systems project sponsored by the Ministry of Science and ICT of the Korean government (2020M2D5A1078126).

REFERENCES

[1] S. Mirshak, W.S. Durant, Towell, Heat flux at burnout, No. DP-355. Du Pont de Nemours (EI) & Co. Savannah River Lab., Augusta, Ga (1959).

[2] M. Kaminaga, K. Yamamoto, Y. Sudo, Improvement of critical heat flux correlation for research reactors using plate-type fuel, Journal of nuclear science and technology 35(12) (1998) 943-951.

[3] M. Kureta, H. Akimoto, Critical heat flux correlation for subcooled boiling flow in narrow channels, International journal of heat and mass transfer 45(20) (2002) 4107-4115.

[4] Kim, Huiyung, et al. "Investigation of the CHF correlation for a narrow rectangular channel under a downward flow condition" International Journal of Heat and Mass Transfer 130 (2019): 60-71.

[5] http://www.matweb.com/search/DataSheet.aspx?MatGUID=6b29957fc95e426d87dff64d67c59f6c. Accessed 1 Apr. 2021.